# Highly Oriented Growth of *p*-Sexiphenyl Molecular Nanocrystals on Rubbed Polymethylene Surface

**Wei-Shan Hu,[‡] Yen-Fu Lin,[§] Yu-Tai Tao,*[,†,‡] Yao-Jane Hsu,[||] and Der-Hsin Wei[||]**

*Institute of Chemistry, Academia Sinica, Taipei,115, Taiwan, R.O.C., Department of Chemistry, National Tsing-Hua University, Hsin-chu, Taiwan, R.O.C., Department of Chemistry, National Central University, Chung-li, Taiwan, R.O.C., and National Synchrotron Radiation Research Center, Hsin-chu, 300, Taiwan, R.O.C.*

*Received June 20, 2005; Revised Manuscript Received September 10, 2005*

ABSTRACT: Highly oriented nanocrystals of *p*-sexiphenyl molecules were prepared by thermal evaporation of this material on a rubbed polymethylene surface. The polymethylene thin film, generated on a gold surface by the gold-catalyzed decomposition of diazomethane, was gently rubbed in a fixed direction with a flannelette cloth to serve as the template for alignment, which induced the in-plane orientation as well as flat-lying geometry of the molecules in contact with the surface. Anisotropic growth from the aligned molecules resulted in oriented molecular crystals. Various techniques, including reflection−absorption IR spectroscopy (RAIRS), near-edge X-ray absorption fine structure (NEXAFS) spectroscopy, grazing incidence X-ray diffraction, and atomic force microscopy were used to elucidate the structural details at the rubbed polymethylene surfaces and the *p*-sexiphenyl crystals deposited on it. The polymethylene chains near the surface were markedly aligned after the rubbing action, with the carbon chain backbones aligned parallel to the rubbing direction. *p*-Sexiphenyl formed nanometer-scale, rodlike molecular crystals, with the long axes of the crystals perpendicular to the rubbing direction. Nevertheless, the molecules in the crystals lay "flat" on the rubbed polymethylene surface, with their long molecular axis parallel to the rubbing direction. Large-scale alignment of highly oriented molecular crystals can be achieved in this manner.

## Introduction

Molecular electronic devices based on organic semiconducting materials have attracted great attention because of their demonstrated potentials in areas such as light-emitting diodes (OLEDs), rectifier, solar cells, etc.[1] The organic semiconducting materials offer the advantages of low-cost and low-temperature processing, and adaptability to large panel and flexible substrates when compared with silicon-based materials. Depending on the application, different film materials and properties are desired. For example, in OLED applications, materials with high luminescent efficiency or charge-transporting ability yet amorphous film-forming property are usually desired.[2] In organic field-effect transistor (OFET) applications, a crystalline film with high field-effect charge mobility and on/off ratio is actively pursued.[3] The charge conduction in semiconducting organic materials, although in general inferior to that of inorganic semiconductors, depends very much on the weak electronic interactions among discrete molecular components so that a strong $\pi-\pi$ stacking in an ordered array such as in a single crystal would most favor the charge migration.[4] The charge mobility is direction-dependent, that is, with the direction along $\pi-\pi$ stacking favored.[5] In the case of deposited thin films, where polycrystalline films are usually obtained, numerous grain boundaries and discontinuities are present. The charge conduction is greatly retarded due to these defects or inhomogeneous regions. While the size of the crystallites can be increased by choosing proper deposition conditions, say, substrate temperature, a compromise between crystal size and grain boundary resistance may exist as the contact between larger crystals will decrease. For a field-effect transistor utilizing polycrystalline organic thin film as the active channel material, an optimization in the film morphology as well as the uniform alignment of the crystallites will be desirable to achieve higher efficiency. Also, depending on the device structure, a control of the alignment of semiconducting molecules relative to the substrate surface and the electrodes is important.

Specific alignment of organic molecules with respect to a substrate surface is well documented. For example, rodlike conjugate aromatic molecules, such as pentacene or α-sexithiophene, deposited on oxidized silicon are known to "stand up" on the surface,[6] whereas the same film deposited on metals or graphite are "lying down" or parallel to the surface.[7] Yet for α-sexithiophene on $SiO_2$, a conversion from a "flat-lying" to an "upright" arrangement with increasing layer thickness was reported.[8] Deposition temperature can also have a major effect on the orientation, so that *p*-sexiphenyl deposited on a KCl(001) single crystal at 20 °C led to parallel alignment, whereas deposition at 150 °C on the same substrate resulted in perpendicular alignment.[9] The reasons for various alignment effects and the kinetic process involved are not fully understood. A balance among intermolecular, $\pi$ surface−substrate, and molecular edge−substrate interactions, as well as entropies of packing may be involved. In-plane molecular alignment is another important aspect of orientation control. The most notable example is the alignment of liquid crystalline molecules on a rubbed polyimide surface. Both "groove effect" and specific electronic interactions between liquid crystals and the aligned polymer chains

* Corresponding author. E-mail: ytt@chem.sinica.edu.tw. Telephone: +886-2-27898580. Fax: +886-2-27831237.
[†] Institute of Chemistry, Academia Sinica.
[‡] Department of Chemistry, National Tsing-Hua University.
[§] Department of Chemistry, National Central University.
[||] National Synchrotron Radiation Research Center.

10.1021/ma051298m CCC: $30.25 
Published on Web 10/14/2005

have been suggested as the cause of alignment.[10] Oriented growth of molecular crystals on friction-transferred polymer substrates, such as poly(tetrafluoroethylene)[11] and poly(*p*-phenylene),[12] is also well documented. Two main models, the molecular-scale epitaxy model and the mesoscopic-scale topography model, have been proposed to interpret the growth mechanism.[13] α-Sexithiophene was reported to form a flat-lying, biaxially anisotropic layer on a stretched polyethylene.[14] An in-plane orientation was induced by rubbing of the predeposited film followed by further deposition.[15]

In this paper, we report the alignment effect of polymethylene, $-(CH_2)_n-$, and rubbed polymethylene on the packing orientation of *p*-sexiphenyl molecular crystals. *p*-Sexiphenyl is examined as a representative of the long conjugate aromatic semiconducting molecules. The oriented growth of *p*-sexiphenyl was examined previously on friction-transferred poly(*p*-phenylene)[12] and rubbed thin film of the molecules themselves.[15] The polymethylene used here is structurally similar to that of polyethylene and is readily formed from diazomethane via gold-catalyzed polymerization.[16] Rubbing of the low $T_g$ polymer was effected with a flannelette cloth. Reflection−absorption IR spectroscopy (RAIRS), near-edge X-ray absorption fine structure (NEXAFS) spectroscopy, grazing incidence X-ray diffraction, and atomic force microscopy were used to characterize the structure of the vapor-deposited *p*-sexiphenyl films. It is concluded that rubbing resulted in the alignment of the hydrocarbon chains near the surface, which induced the contacting molecules to align along the polymer chains. The crystallites nevertheless grow into rods, with the long axes perpendicular to the polymer chains.

## Experimental Section

**Sample Preparation.** The gold substrate was prepared by thermal evaporation of high-purity gold (99.99%) onto a one-side polished silicon (100) wafer. The wafer was precleaned by a Piranha solution ($H_2SO_4/H_2O_2$ = 4:1). To increase the adhesion between the gold and the silicon wafer, a layer of 13 nm chromium film was deposited on the silicon wafer prior to the deposition of 130 nm of gold.

The polymethylene films were prepared by gold-catalyzed decomposition of diazomethane as previously reported.[16] Gold substrates were placed in an ethereal solution of diazomethane for a period of time at 0 °C. The substrates were taken out of solution at the end of the immersion, washed with pure ether and absolute ethanol, and finally, spin-dried. The thickness of the polymethylene film was determined by a profilometer. Typically, a film with a thickness of ∼250 nm was used. For rubbed polymethylene, the as-prepared film was gently rubbed with a flannelette cloth in a single direction a dozen times.

The *p*-sexiphenyl was synthesized according to literature procedure[17] and purified by sublimation at least twice. The deposition of *p*-sexiphenyl was carried out in a vacuum chamber at room temperature at an evaporation rate of 0.5 nm/s and under a pressure of $<2 \times 10^{-5}$ Torr. The film thickness was monitored by a quartz crystal thickness monitor.

**Infrared External Reflection Spectroscopy.** Reflection−absorption IR spectra were recorded in single reflection mode with a grazing incidence angle of 86° by using a Digilab FTS 60A Fourier transform infrared spectrometer (Bio-Rad, Cambridge, MA). A liquid-nitrogen-cooled MCT detector was used. Four hundred scans were collected for spectral data processing. The spectra are recorded as a function of reflectivity, $-\log(R/R_0)$, where $R_0$ is the reflectivity of a clean reference gold sample, and $R$ is the reflectivity of polymer- or molecular film-coated gold substrate.

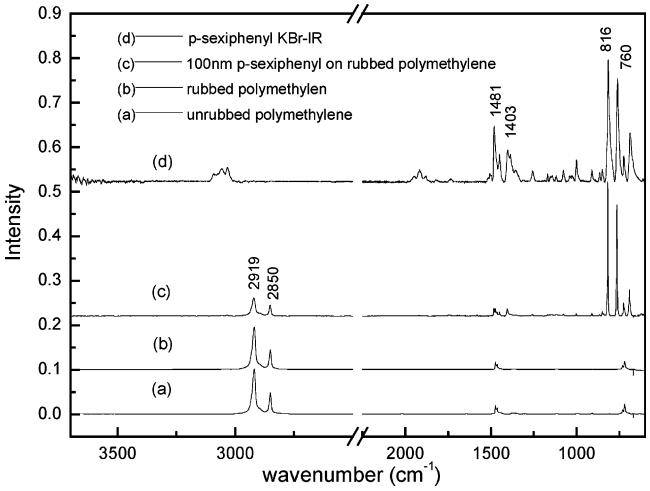


**Figure 1.** Reflection−absorption IR spectra of (a) 250-nm-thick polymethylene film grown on a bare gold surface, (b) the rubbed polymethylene, (c) 100-nm-thick *p*-sexiphenyl thermally deposited on the rubbed polymethylene, and (d) the spectrum of KBr pellet of isotropic *p*-sexiphenyl sample.

**Near Edge X-ray Absorption Fine Structure Spectroscopy.** The near-edge X-ray absorption fine structure (NEXAFS) spectra were taken at the X-ray photoemission electron microscopy (X-PEEM) station at the National Synchrotron Radiation Research Center (NSRRC), Hsin-chu, Taiwan. The *s*- and *p*-polarized radiation with an energy resolution of 100 meV at the carbon *K*-edge and a focused spot size of 0.1 × 1 mm$^2$ was delivered to the sample at a 65° incident angle through an elliptically polarized undulator (EPU5.6) beamline. The sample current was measured with a picoammeter to obtain the NEXAFS spectra in the total electron yield (TEY) mode.

**Grazing Incidence Angle X-ray Diffraction.** X-ray diffraction patterns were obtained at the wiggler 17B beamline of the NSRRC. An incidence X-ray with 8 keV energy and a wavelength of 1.55 Å was used, and a grazing incidence angle below the critical angle of the total reflection from the substrate and above the critical angle for the film was chosen to enhance the sensitivity of measurement.

**Atomic Force Microscopy (AFM).** AFM measurements were carried out under ambient conditions using a Digital Instruments Nanoscope IIIa microscope (Digital Instruments, Santa Barbara, CA) operated in tapping mode. Commercially obtained monocrystalline silicon cantilevers (Nanosensors, Germany) with typical spring constants of 21−78 N/m were used.

## Results and Discussion

**Reflection−Absorption Infrared Spectroscopy.** Reflection−absorption IR spectroscopy provides useful information regarding molecular orientation on a reflective metal surface on the basis of the selection rule that only vibrational modes having their transition dipoles oriented along the surface normal will get excited and result in absorption.[18] An analysis of the relative absorption intensity of various modes and the corresponding transition dipole vectors can generate information on the orientation of a chromophore or a molecule relative to the surface. Figure 1a shows the reflection−absorption IR spectrum of ∼250 nm polymethylene film grown on a bare gold surface. It exhibits typical features expected for extended $-(CH_2)_x-$ chains: 725 cm$^{-1}$ for $CH_2$ rocking and 1470 cm$^{-1}$ for $CH_2$ scissors deformation. The absorptions at 2850 and 2919 cm$^{-1}$ for symmetrical and asymmetrical $CH_2$ stretching vibrations, respectively, indicate the near-crystalline state of the film obtained. Figure 1b shows

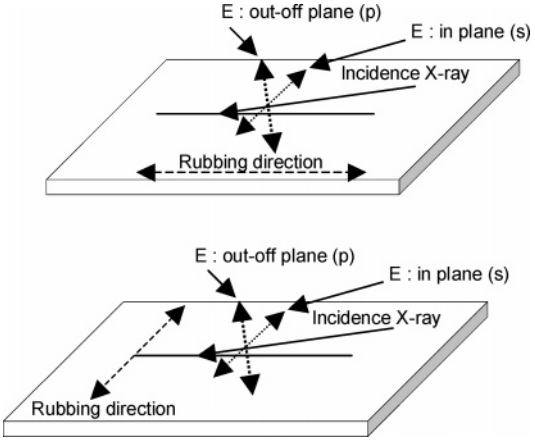


**Figure 2.** The measurement geometry of incident X-ray. The *s*-polarization was aligned either (a) parallel or (b) perpendicular to the rubbing direction.

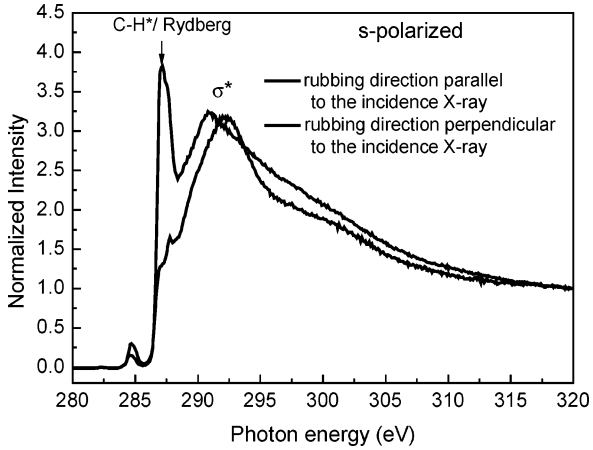


**Figure 3.** The NEXAFS spectra of *s*-polarized X-ray measured for the rubbed polymethylene with *E* vector parallel and perpendicular to the rubbing direction.

the spectrum for the rubbed polymethylene, which is very similar to the unrubbed one. In contrast to the NEXAFS results (vide supra), the reflection IR did not yield information on the structural change upon rubbing of the surface, presumably because of the greater probing depth of IR[19] and the very superficial change as a result of rubbing. This is in agreement with the X-ray scattering study of the effect of rubbing of polyimide film,[20] that is, only a very thin surface region (about 5 nm thick) are aligned upon rubbing. Figure 1c shows the spectrum for a 100-nm-thick layer of *p*-sexiphenyl thermally deposited on the rubbed polymethylene. Also included is the spectrum prepared from a KBr pellet of isotropic *p*-sexiphenyl sample for comparison. The most prominent feature for the deposited film is the strong absorptions at 760 and 816 $cm^{-1}$, respectively,[21] which are attributed to the out-of-plane bending vibrations of the phenyl ring C−Hs. These vibration modes have their transition dipoles aligned normal to the ring plane.[21] The vibration modes associated with ring stretches (occurring at ∼1481 $cm^{-1}$ for the mode 19a and at ∼1403 $cm^{-1}$ for the mode 19b) and aromatic C−H stretches (at ∼3061 $cm^{-1}$ for the mode 20a and 3027 $cm^{-1}$ for the mode 20b), which have their transition dipoles parallel to the ring plane along the long axis and short axis, respectively,[21] are much weaker compared with that of the spectrum of isotropic sample of *p*-sexiphenyl. The ratios of IR absorption intensity $I_{816}/I_{1481} \approx 2.2$ and $I_{816}/I_{1403} \approx 3.6$ for KBr−IR sample became 17.8 and 16.8, respectively, for the 100-nm-thick *p*-sexiphenyl sample. From the orthogonal relationship of these vibrational modes, the long axis of the molecule is estimated to be nearly parallel to the surface, and the short axis of the molecule is off more from the surface, presumably due to the herringbone packing of the aromatic rings (vide infra).

**Near-Edge X-ray Absorption Fine Structure Spectroscopy.** To further explore the orientational details of the rubbed polymethylene as well as the deposited film, linear polarization-dependent near-edge X-ray absorption fine structure (NEXAFS) measurements were carried out on the films. The *s*-polarization of the incident X-ray was aligned either parallel or perpendicular to the rubbing direction, as indicated in Figure 2a and b. The NEXAFS spectra of *s*-polarized X-ray measured for rubbed polymethylene in both directions are shown in Figure 3. A much enhanced C−H*/Rydberg resonance[22] at 287 eV was observed

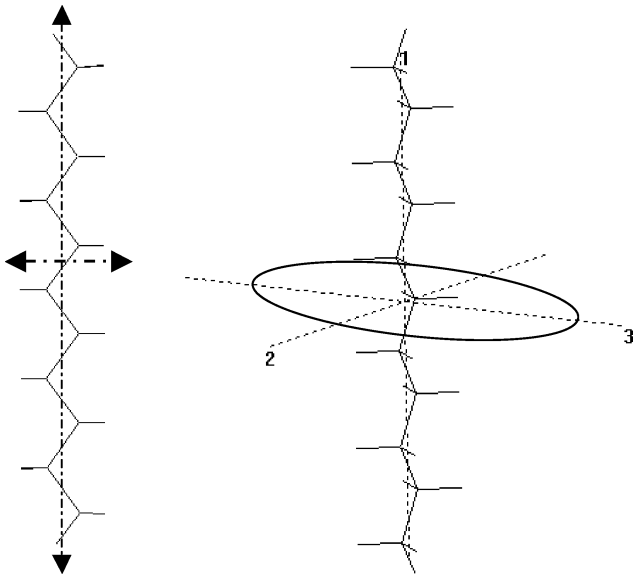


**Figure 4.** The two possible alignments of polymethylene chains, with the plane containing C−C−C backbone either parallel or perpendicular to the surface. The C−H bonds are pointing "left and right" or "up and down" accordingly.

when the *s*-polarized incidence X-ray irradiated at the polymethylene surface along the rubbing direction. In this configuration, the *E* vector is perpendicular to the rubbing direction. The broad band appearing in the region 291−315 eV is characterized as $\sigma^*$ resonances.[22] In contrast, the C−H*/Rydberg resonance was dramatically reduced when the *s*-polarized X-ray is directed perpendicular to the rubbing direction, a condition under which the *E* vector is parallel to the rubbing direction. The $\sigma^*$ resonances gave similar intensity to that the above. These NEXAFS results strongly suggest that the trans zigzag C−C−C backbone chains were highly oriented after rubbing and are aligned parallel to the rubbing direction. The C−H bonds of polymethylene chains were pointing left and right or up and down and perpendicular to the C−C backbone chain, as shown in Figure 4. When the X-ray is directed along the rubbing direction and, thus, the backbone direction, the $E_s$ is parallel to the C−H bonds and an enhancement in the C−H* transition is expected. When the X-ray is directed perpendicular to the rubbing direction, the $E_s$ is orthogonal to the C−H bonds and the C−H* transition is minimized.

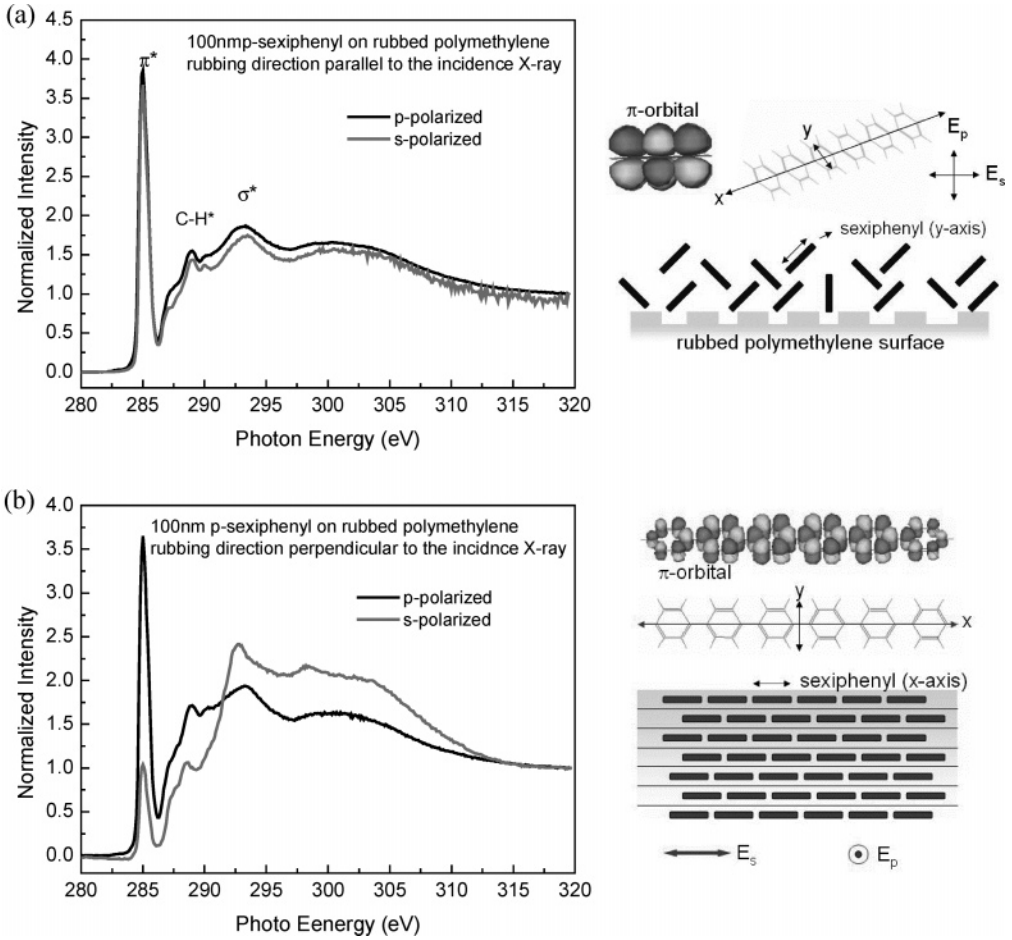


**Figure 5.** The NEXAFS spectra of 100-nm-thick *p*-sexiphenyl on the rubbed polymethylene surface. The *s*- and *p*-polarized X-ray with an incident angle of 65° from the surface normal and aligned (a) parallel to the rubbing direction, or (b) perpendicular to the rubbing direction.

Figure 5 shows the NEXAFS measurements for a 100-nm-thick *p*-sexiphenyl film deposited on the rubbed polymethylene surfaces. The NEXAFS spectra of the *s*- and *p*- polarized X-ray with an incident angle of 65° from the surface normal and aligned parallel to the rubbing direction are shown in Figure 5a. The spectra recorded with the two polarizations are quite similar, and no dichroism was found. In contrast, a prominent difference between the spectra for *s*- and *p*-polarization was observed when the incident X-ray was directed perpendicular to the rubbing direction, as shown in Figure 5b. The $\pi^*$ resonance of phenyl rings at 285 eV was strongly enhanced in the *p*-polarization spectrum. In the *s*-polarization, the $\pi^*$ resonance is reduced, whereas the $\sigma^*$ resonance at 293 eV is enhanced. The results can be rationalized by highly oriented *p*-sexiphenyl molecules with their long molecular axes aligned parallel to the rubbing direction and crystallized in a herringbone packing. With such an alignment in a multilayer film, the *p*-orbitals of the phenyl rings will point perpendicular to the rubbing direction yet alternate toward left and right along the layer direction due to the herringbone packing. The much-reduced intensity for the $\pi^*$ resonance in *s*-polarization mentioned above is due to a perpendicular relationship between the $E_s$ and the *p*-orbitals.

**X-ray Diffraction.** The *p*-sexiphenyl is a straight rigid rod molecule with high crystallinity. The *p*-sexiphenyl crystallizes in monoclinic form, having lattice constants of $a$ = 8.091 Å, $b$ = 5.568 Å, $c$ = 26.241 Å,

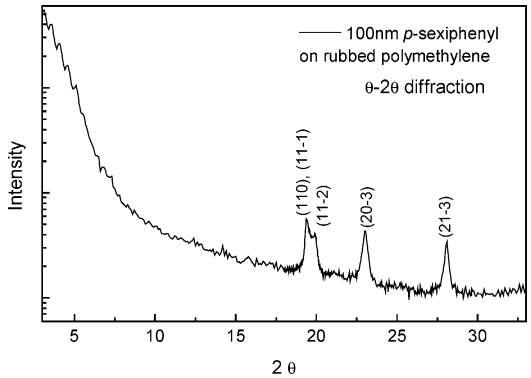


**Figure 6.** X-ray diffraction pattern of 100-nm-thick *p*-sexiphenyl film on the rubbed polymethylene surface.

and $\beta$ = 98.17°, with the space group $P2_1/c$.[23] The molecules align, but slightly incline relative to the *c*-axis of the unit cell. In contrast to a free molecule, which has space for rotation of individual phenyl rings, the *p*-sexiphenyl molecules in a crystal state is constrained into a planar form with six phenyl rings situated in the same plane.[23] X-ray diffraction was carried out on a 100-nm-thick *p*-sexiphenyl sample deposited on a rubbed polymethylene surface. As shown in Figure 6, the diffraction peaks correspond to lower *d* spacings: ~4.57 Å at 19.4°, ~4.46 Å at 20.04°, ~3.86 Å at 23.09°, and ~3.17 Å at 28.16°, which are assigned to the diffraction planes of (110), (11−1), (11−2), (20−3), and (21−3), respectively. Further studies of the preferred orientation

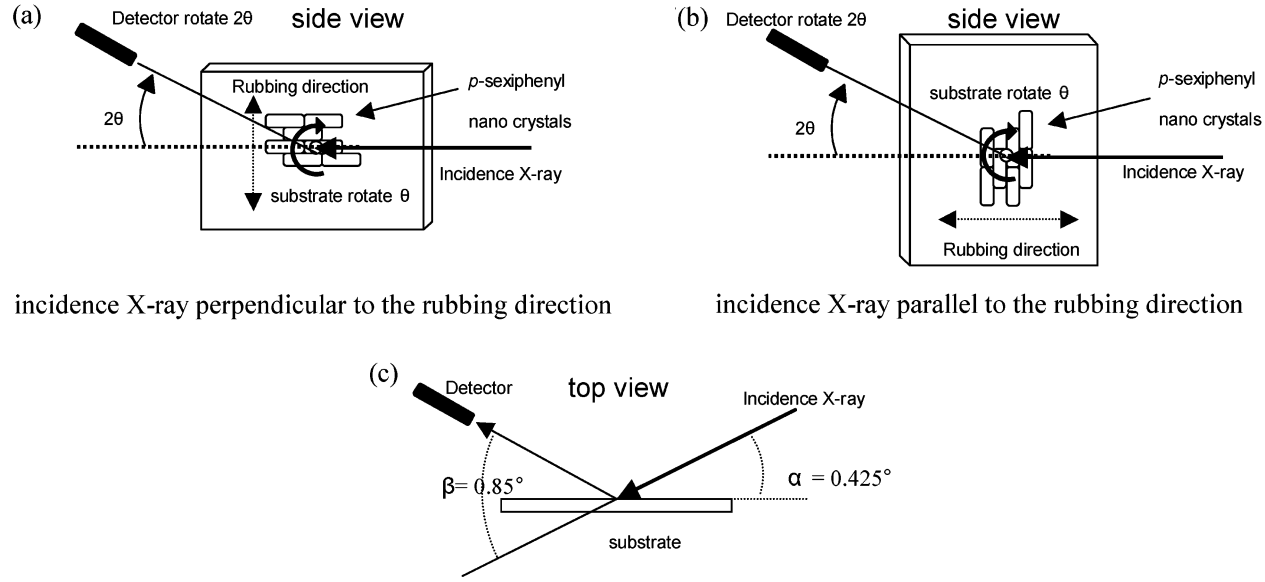


**Figure 7.** Geometries of in-plane grazing incidence X-ray diffraction experiments. The grazing incidence X-ray with an incidence angle of 0.425° aligned (a) perpendicular to the rubbing direction, or (b) parallel to the rubbing direction. (c) Top view of the measurement alignment.

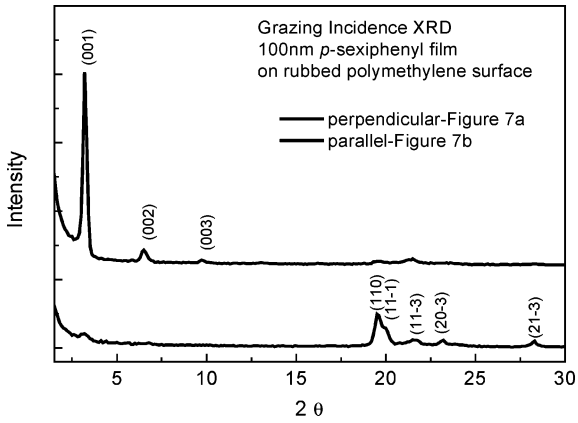


**Figure 8.** The in-plane grazing incidence XRD pattern of 100-nm-thick *p*-sexiphenyl on rubbed polymethylene with incidence X-ray parallel and perpendicular to the polymer rubbing direction.

of the *p*-sexiphenyl molecular crystals were carried out by using the grazing incidence X-ray diffraction analysis. To measure the preferred alignment for (001) diffraction plane of *p*-sexiphenyl crystals, two kinds of in-plane orientation measurement were carried out: one with incident X-ray aligned perpendicular to the rubbing direction with an incidence grazing angle of 0.425° and followed by the in-plane $\theta-2\theta$ scan, the other with the incidence X-ray aligned parallel to the rubbing direction with the same grazing angle and followed by the in-plane $\theta-2\theta$ scan. The geometries from which the spectra were recorded are shown in Figure 7. The results of in-plane X-ray grazing incidence diffraction are shown in Figure 8. The (001), (002), (003) diffraction peaks were found at $2\theta$ values around 3.2°, 6.5°, and 9.7°, respectively, when the incidence X-ray is perpendicular to the rubbing direction. The results strongly suggest that the (001) plane of the *p*-sexiphenyl nanocrystals aligns parallel to the rubbing direction of the film. On the other hand, no (001) diffraction peak was found when the incidence X-ray was parallel to the rubbing direction. Instead, diffraction peaks corresponding to much lower *d* spacings of ~4.5Å at 19.5°, ~4.1 Å at 21.5°, ~3.8 Å at 23.2°, and ~3.14 Å at 28.3° were observed, which are attributed to the diffraction planes of (110), (11−1), (11−3), (20−3), and (21−3), respectively. These results imply that the *p*-sexiphenyl nanocrystals were aligned with their lower *d* spacing planes perpendicular to the rubbing direction, with an interplanar spacing around 3 Å.These results together strongly suggest that the flat-lying *p*-sexiphenyl molecules have a preferred orientation with their long molecular axis parallel to the rubbing direction.

**Atomic Force Microscopy.** The AFM images of polymethylene films as prepared on Au, polymethylene film after rubbing, as well as 100-nm-thick film of *p*-sexiphenyl deposited on the rubbed polymethylene surface are shown in Figure 9. Figure 9a and b show the topography of polymethylene grown on a Au surface appear to give sphere-like clusters with an average diameter around 80 nm. The surface exhibits a root-mean-square roughness of 22.7 nm. The film after rubbing with a flannelette cloth in a fixed direction, on the other hand, shows parallel stripes along the rubbing direction (Figure 9c and d). The roughness of the rubbed polymethylene surface was greatly reduced, to a root-mean-square roughness of 8.69 nm. Some hollow defects were found on the rubbed polymethylene surface, probably due to the rough morphology of the original polymethylene film. The AFM micrographs of 100-nm-thick, thermally evaporated *p*-sexiphenyl film on the rubbed polymethylene are shown in Figure 10a and b. Rod-shaped crystallites of *p*-sexiphenyl with an average size of about 110 nm long and 30 nm in width are observed. A clearly preferred orientation of the crystallites was found with their long crystal axes aligned *perpendicular* to the rubbing direction (the arrow direction). For comparison, a gold surface modified with a self-assembled monolayer of eicosanethiol was used as a reference substrate for depositing *p*-sexiphenyl film. The X-ray diffraction and reflection IR suggest that the *p*-sexiphenyl crystals are lying flat like on a polymethylene surface. The AFM image shows similar rodlike crystallites that are randomly oriented on the SAM-covered Au surface, Figure 10c.

The polarization-dependent NEXAFS and X-ray diffraction above clearly suggest that the long molecular

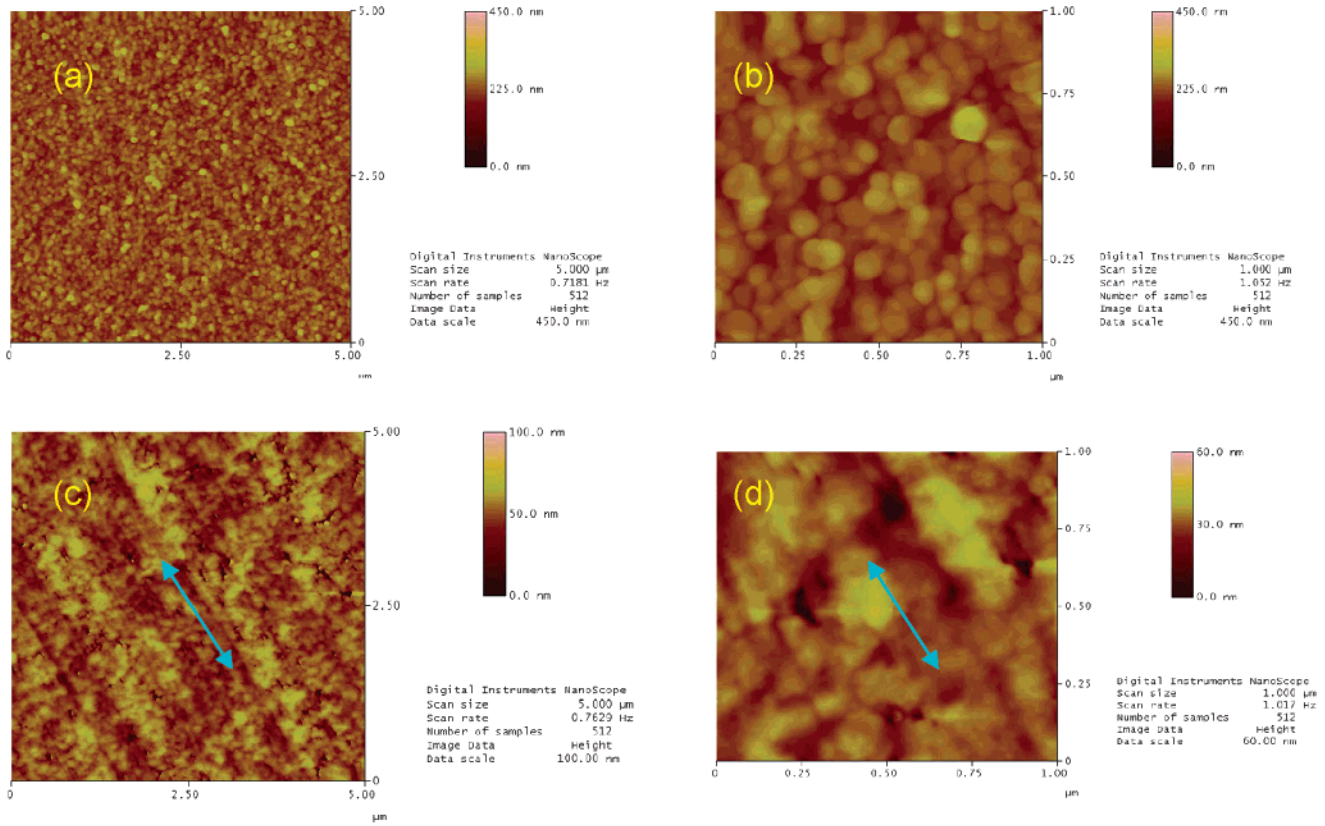


**Figure 9.** AFM images of polymethylene grown on Au: (a) 5 $\mu$m field of view, (b) 1 $\mu$m field of view. Rubbed polymethylene surface: (c) 5 $\mu$m field of view, (d) 1 $\mu$m field of view; the arrow indicates the rubbing direction.

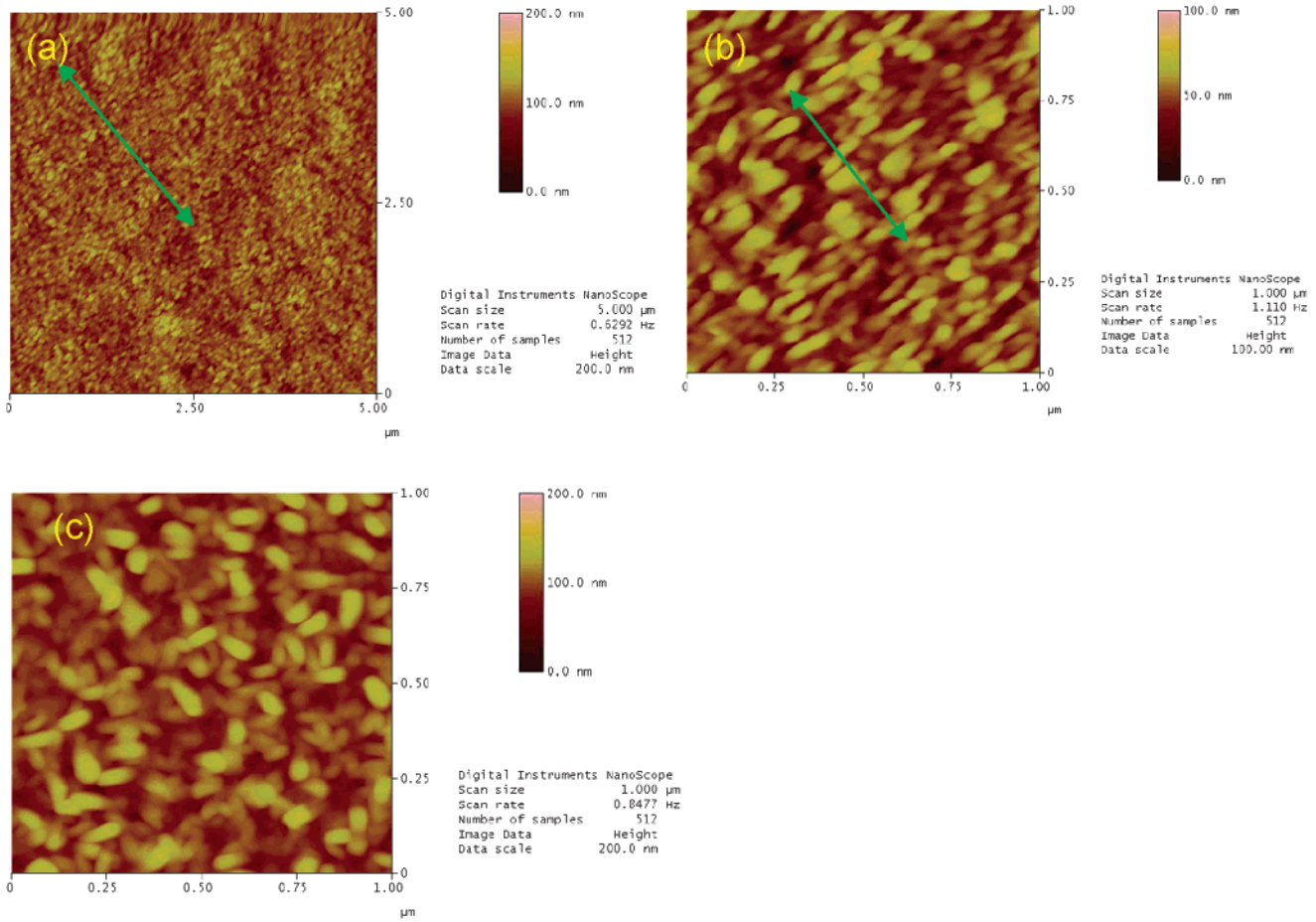


**Figure 10.** AFM images of 100-nm-thick *p*-sexiphenyl film on rubbed polymethylene surface: (a) 5 $\mu$m field of view, (b) 1 $\mu$m field of view, the arrow indicates the rubbing direction, (c) 100-nm-thick *p*-sexiphenyl film deposited on *n*-eicosanethiol-covered gold.

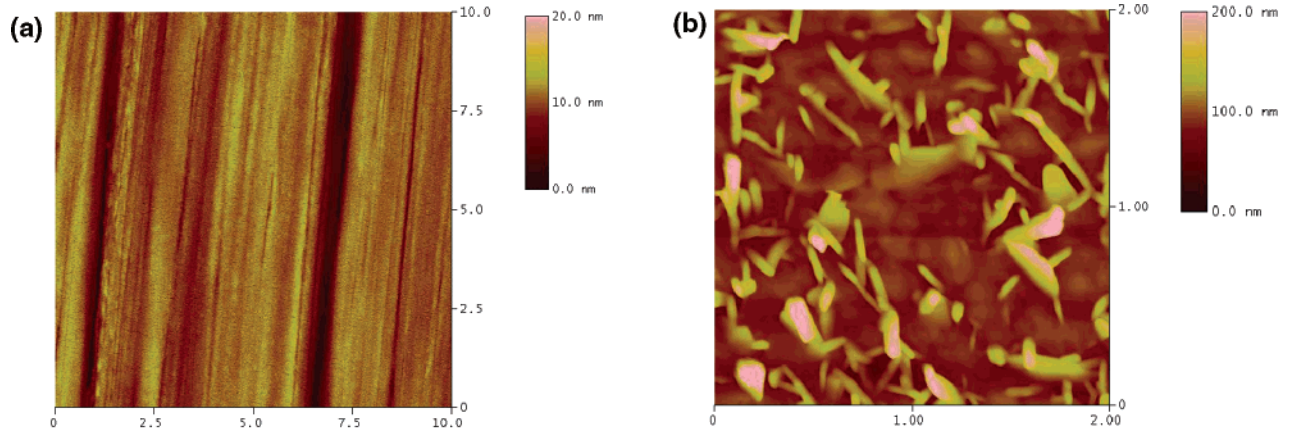


**Figure 11.** AFM images of (a) 30 nm of gold deposited on the rubbed polymethylene, (b) 100-nm-thick *p*-sexiphenyl film deposited on the grooved gold surface.

axes of *p*-sexiphenyl align with the rubbing direction. The AFM image shows that the long axes of the crystals align orthogonally to the rubbing direction. This concludes that the long axis of the crystal is different from the long axis of the molecule. It also suggests the crystal grows more in the lateral direction of the molecule rather than in the longitudinal direction.

To differentiate the effect of grooves and molecular chains in directing the alignment of the arriving *p*-sexiphenyl, a "grooved" gold surface was prepared by evaporating a 30-nm-thick layer of gold on the rubbed polymethylene. As shown in Figure 11a, the surface resembles that of the rubbed polymethylene surface with stripes along the rubbing direction. Figure 11b shows the AFM image of 100-nm-thick *p*-sexiphenyl deposited on the grooved gold surface. It resembles the film deposited on a clean gold surface and on a SAM-covered gold surface (Figure 10c). Thus, randomly oriented crystallites with flat-lying molecular packing were obtained. This would eliminate the role of grooves in aligning the molecules. The electronic interaction between the aligned hydrocarbon chains and the aromatic moiety dictates the initial orientation of the molecules.

The various techniques here corroborate the mechanism of the alignment of the *p*-sexiphenyl molecules on a rubbed polymethylene surface. Rubbing of a linear hydrocarbon polymer results in a general alignment of the hydrocarbon backbone near the top of the surface, in addition to the nanoscale grooves, along the rubbing direction.[20] Vapors of long, rodlike aromatic molecules arrive at the surface and interact with the aligned hydrocarbon surface, possibly through a C−H/$\pi$ interaction.[24] The interaction maximizes with the molecule lying parallel to the chain. The molecule−substrate interaction is strong enough to dictate the rest of nucleation process: the crystal maintains the "flat-lying" alignment of the molecules and grows faster in the lateral direction than the longitudinal direction[25] to lead to long rods oriented orthogonal to the groove direction. Thus, the distinct directions of the crystallites and the grooves result from different growth kinetics of various faces of the crystal. The grooves play no role in affecting the orientation of the crystals.

It is noted that, in the deposition of related α-sexithiophene onto a silica surface, the molecules were parallel to the surface at submonolayer coverage, yet all changed to the vertical orientation after formation of the first monolayer was completed.[8] The switching of orientation may have to do with the interaction energy involved in the substrate/monolayer interface. With a weaker interaction, a perpendicular orientation is always favored, even if the initial orientation is parallel. With a stronger interaction, the initial parallel orientation retains and dictates the alignment for additional layers. Compared to the alignment of *p*-sexiphenyl on friction-transferred poly(*p*-phenylene)[12] or rubbed *p*-sexiphenyl film,[15] the alignment interaction is due to the saturated hydrocarbon chain and the $\pi$ system. This C−H/$\pi$ "hydrogen bonding" is weaker than the $\pi-\pi$ stacking interaction, yet sufficient to retain the *p*-sexiphenyl molecules in a "flat lying" orientation when more molecules are deposited on top. The moderate interaction may allow modulation of orientation (change from flat-lying to straight up) through temperature control in view of the temperature effect on the orientation of *p*-sexiphenyl film on KCl(100) crystal.[9]

## Conclusion

In conclusion, we showed here that the orientation of a long conjugate aromatic molecule such as *p*-sexiphenyl within a thin film can be controlled in three directions by using a rubbed polymethylene surface. The interaction between the $\pi$ surface and the stretched hydrocarbon chain locks the molecule into a flat-lying and parallel-to-the-chain direction. The aligned molecules direct the growth of the crystals into highly oriented crystallites, with the long axes of the molecules parallel to the rubbing direction and the long axes of the crystal perpendicular to the rubbing direction. A similar alignment effect was also observed for α-sexithiophene. Integration of the orientation control into a device fabrication process and the possible direction-dependent electric conductance is being investigated.

**Acknowledgment.** The research was supported by National Science Council, Taiwan, Republic of China and Academia Sinica, Republic of China.

## References and Notes

(1) Kelley, T. W.; Baude, P. F.; Gerlach, C.; Ender, D. E.; Muyres, D. Haase, M. A.; Vogel, D. E.; Theiss, S. D. *Chem. Mater.* **2004**, *16*, 4413.
(2) Shirota, Y. *J. Mater. Chem.* **2000**, *10*, 1.
(3) (a) Horowitz, G. *J. Mater. Chem.* **1999**, *9*, 2021. (b) Katz, H. E.; Bao, Z. *J. Phys. Chem. B* **2000**, *104*, 671.
(4) Janzen, D. E.; Burand, M. W.; Ewbank, P. C.; Pappenfus, T. M.; Higuchi, H.; da Silva Filho, D. A.; Young, V. G.; Brédas, J.-L.; Mann, K. R. *J. Am. Chem. Soc.* **2004**, *126*, 15295.

(5) (a) van de Craats, A. M.; Stutzmann, N.; Bunk, O.; Nielsen, M. M.; Watson, M.; Müllen, K.; Chanzy, H. D.; Sirringhaus, H.; Friend, R. H. *Adv. Mater.* **2003**, *15*, 495. (b) Rochefort, A.; Martel, R.; Avouris, P. *Nano Lett.* **2002**, *2*, 877.
(6) (a) Shtein, M.; Mapel, J.; Benziger, J. B.; Forrest, S. R. *Appl. Phys. Lett*. **2002**, *81*, 268. (b) Dimitrakopoulos, C. D.; Brown, A. R.; Pomp, A. *J. Appl. Phys*. **1996**, *80*, 2501.
(7) (a) Schroeder, P. G.; France, C. B.; Park, J. B.; Prkinson, B. A. *J. Appl. Phys*. **2002**, *91*, 3010. (b) France, C. B.; Parkinson, B. A. *Appl. Phys. Lett*. **2003**, *82*, 1194. (c) Kang, J. H.; Zhu, X. Y. *Appl.* Phys. Lett. **2003**, *82*, 3248. (d) Cvetko, D.; Danieli, R. *Synth. Met*. **1996**, *76*, 173. (e) Hu, W. S.; Tao, Y. T.; Hsu, Y. J.; Wei, D. H.; Wu, Y. S. *Langmuir* **2005**, *21*, 2260. (f) Harada, Y.; Ozaki H.; Ohno, K. *Phys. Rev. Lett.* **1984**, *52*, 2269.
(8) (a) Loi, M. A.; Como, E. D.; Dinelli, F.; Murgia, M.; Zamboni, R.; Biscarini, F. and Muccini, M. *Nat. Mater.* **2005**, *4*, 81. (b) Ivanco, J.; Winter, B.; Netzer, F. P.; Ramsey, M. G. *Adv. Mater.* **2003**, 15, 1812.
(9) Yanagi, H.; Olamoto, S. *Appl. Phys. Lett*. **1997**, *71*, 2563.
(10) (a) Berreman, D. W. *Phys. Rev. Lett.* **1972**, *28*, 1683. (b) Zhu, Y. M.; Wang, L.; Lu, Z. H.; Wei, Y.; Chen, X. X.; Tang, J. H. *Appl. Phys. Lett*. **1994**, *65*, 49. (c) van Aerle, N. A. J. M.; Tol, A. J. W. *Macromolecules* **1994**, *27*, 6520. (d) Geary, J. M.; Goodby, J. W.; Kmetz, A. R.; Patel, J. S. *J. Appl. Phys.* **1987**, *62*, 4100.
(11) Wittman, J. C.; Smith, P. *Nature* **1991**, *352*, 414.
(12) Yase, K.; Han, Y. M.; Yamamoto, K.; Yoshida, Y.; Takada, N.; Tanigaki, N. *Jpn. J. Appl. Phys.* **1997**, *36*, 2843.
(13) Damman, P.; Coppée, S.; Geskin, V. M.; Lazzaroni, R. *J. Am. Chem. Soc.* **2002**, *124*, 15166.
(14) Oelkrug, D.; Egelhaaf, H. J.; Haiber, J. *Thin Solid Films* **1996**, *284*−*285*, 267.
(15) (a) Era, M.; Tsutsui, T.; Saito, S. *Appl. Phys. Lett.* **1995**, *67*, 2436. (b) Erlacher, K.; Resel, R.; Keckes, J.; Meghdadi, F.; Leising, G. *J. Cryst. Growth*, **1999**, *206*, 135. (c) Chen, X. L.; Lovinger, A. J.; Bao, Z.; Sapjeta, J. *Chem. Mater*. **2001**, *13*, 1341.
(16) Seshadri, K.; Atre, S. V.; Tao, Y. T.; Lee, M. T.; Allara, D. *J. Am. Chem. Soc.* **1997**, *119*, 4698.
(17) Kovacic, P.; Lange, R. M. *J. Org. Chem*. **1964**, *29*, 2416.
(18) Parikh, A. N.; Allara, D. L. *J. Chem. Phys.* **1992**, *96*, 927.
(19) The reflection IR probes the whole thickness of the film, yet the NEXAFS is known to probe only the top tens of nanometers. Stöhr, J.; Anders S. *IBM J. Res. Dev.* **2000**, *44*, 535.
(20) Toney, M. F.; Russell, T. P.; Logan, J. A.; Kikuchi, H.; Sands, J. M.; Kumar, S. K. *Nature*, **1995**, *374*, 709.
(21) Varsanyi, G. *Vibrational Spectra of Benzene Derivatives*; Academic Press: New York, 1974.
(22) Stöhr, J. *NEXAFS Spectroscopy*; Springer: Berlin, 1991.
(23) (a) Baker, K. N. Fratini, A. V.; Resch, T.; Knachel, H. C.; Adams, W. W.; Socci, E. P.; Farmer, B. L. *Polymer*, **1993**, *34*, 1571. (b) Toussaint, C. J. *Acta Crystallogr.* **1966**, *21*, 1002.
(24) Nishio, M.; Hirota, M.; Umezawa, Y. *The CH/π Interaction*; Wiley-VCH: New York, 1998.
(25) West, A. R. In *Solid State Chemistry and Its Applications*; John Wiley & Sons: 1984; Chapter 2, p 12.

MA051298M